# GEO-LOCATION ESTIMATION FROM ELECTRICAL NETWORK FREQUENCY SIGNALS

*Ravi Garg, Adi Hajj-Ahmad, and Min Wu*

{ravig, adiha, minwu}@umd.edu
University of Maryland, College Park, MD, USA.

**ABSTRACT**

Electric Network Frequency (ENF) fluctuations based forensic analysis is an emerging way for such multimedia authentication tasks as time-of-recording estimation, timestamp verification, and clip insertion/deletion forgery detection. ENF fluctuates due to dynamic changes in load demand and power supply, and these fluctuations travel over the power lines with a finite speed. In this paper, experiments are conducted on ENF data collected across different locations in the eastern grid of the United States to understand the relationship between the signals recorded at the same time at these locations. Based on these experiments, a signal processing mechanism is developed to demonstrate that ENF fluctuations across different locations exhibit a measure of similarity with each other, which is proportional to the distance between the locations. Such observations motivated a location estimation protocol based on the similarity of ENF signals with respect to anchor nodes. Under certain conditions, the proposed protocol is shown to provide an estimation accuracy of 90%. Challenges in the application of ENF signal analysis for location of recording estimation of multimedia signal are also discussed.

## 1. INTRODUCTION

Advancement in multimedia technologies has given rise to proliferation of such recording devices as voice recorders, camcorders, digital cameras, etc. A huge amount of digital information created using these devices can be stored on disks or uploaded on such social media platforms as YouTube and Facebook. Metadata describing such important information as the time and the place of recording may be manually added or embedded into a media recording using built-in clocks and GPS in the recording devices. However, digital tools can be used to modify the stored information. Developing forensic tools to authenticate multimedia recordings using an environmental signature, known as Electrical Network Frequency (ENF) signal, which emanates from power networks is an active area of research [1] [2].

ENF is the supply frequency of electric power in distribution networks, and its nominal value is 50 or 60 Hz depending on the geographic location. An important property of the ENF signal is that its value fluctuates around the nominal value: on the order of approximately 50-100 mHz in the United States. These fluctuations are due to variations in the load on the power grid and can be considered as occurring at random. The randomly varying ENF signal is embedded into audio recordings due to electromagnetic interference from nearby power lines in audio [1], and in video recordings due to invisible flickering of electric powered indoor lightings [2]. This property of the ENF signal has enabled its use in media forensic analysis, particularly for timestamp authentication and forgery detection.

The ENF signal is extracted from a recording by means of filtering operations followed by instantaneous frequency estimation. ENF can be estimated using Fourier transform based frequency estimation methods as described in [2]. For timestamp authentication and verification, similarity between the ENF signals extracted from multimedia and power databases at the corresponding time can be measured by means of the Normalized Cross-Correlation (NCC) coefficient. A high value of NCC indicates the time at which the recording took place. High resolution frequency estimation methods such as MUSIC and ESPRIT have been shown to provide better instantaneous frequency estimation of the ENF signal for short segments and in the presence of higher noise levels, as compared with the Fourier transform based methods [3]. The performance of ENF matching of two signals is further improved by considering an autoregressive model of the signal [4]. Based on this model, matching the two ENF signals by estimating the correlation coefficient between the corresponding "innovations" sequences provides a higher confidence in time-of-recording estimation and verification.

Most of the existing research has focused on utilizing the ENF signal as a timestamp for multimedia recordings. An important intriguing question that is still unanswered in the literature is: "can the ENF signal be used to estimate or verify the place of recording of an audio or a video recording?" An answer in affirmative can pave a way towards the potential usage of ENF signal analysis in automatic geo-tagging of multimedia data uploaded on YouTube and Facebook in addition to numerous forensic and law enforcement applications.

At an inter-grid level, it may be possible to differentiate between the recordings conducted across different grids, as the fluctuations in the ENF signal are typically different at the same time across independently operated grids. At an intra-grid level, most of the existing work has assumed that the ENF signals across an interconnected power grid are similar at the same time. However, minor variations are likely to be present in the frequency fluctuations at different locations due to local changes in the load on the grid and the finite propagation speed of the effects of such load changes to other parts of the grid [5]. In this paper, we study such effects by conducting experiments on the ENF data collected from different locations within the eastern grid of the United States. As it will be shown later in the paper, there exists differences among simultaneous ENF signals extracted from recordings taken in different locations within the same interconnected power grid. Our study here builds a foundation to design a localization protocol based on a method of half-plane intersection to estimate the location of recordings. The challenges arising due to the noisy nature of the ENF signal from multimedia recordings are also discussed.

## 2. PROPAGATION MECHANISM OF ENF SIGNAL

The fluctuations in the ENF signal in the same grid are due to the dynamic nature of the load on the grid. Power demand and supply in a given area follow a cyclic pattern. For example, demand increases during evening hours in a residential neighborhood, as people switch on air-conditioning and other power units. For robust operation of the grid, any load change is regulated by a control mechanism [6]. An increase in the load causes the supply frequency to drop temporarily; the control mechanism senses the frequency drop and starts drawing power from adjoining areas to compensate for the increased demand. As a result, the load in adjoining areas also increases, which leads to a drop in the instantaneous supply frequency, and the overall power supply will be driven up to compensate the rising load which leads to a drop in the instantaneous supply frequency in those regions. A similar mechanism is used to compensate for an excess supply of power flow that leads to a surge in supply frequency.

A small change in the load in a given area may have a localized effect on the ENF in that area. However, a large change such as one caused by a generator failure may have an effect on the whole grid. In the US eastern grid, these changes are known to propagate along the

grid at a typical speed of approximately 500 miles per seconds [5]. We conjecture that load change may introduce location specific signatures in the ENF patterns, and such differences may be exploited to narrow down the location of a recording within the grid. Due to the finite speed of propagation of frequency disturbances across the grid, we anticipate that ENF signals would be more similar for locations close to each other as compared with those farther apart. Such a property of ENF signal propagation across the grid can be potentially used for localization at a finer resolution within a grid by comparing the similarity of the ENF signal in question with ENF databases that may be available for a set of locations.

## 3. LOCATION DEPENDENCE OF ENF SIGNALS

As a first step to explore the availability of location dependent properties of the ENF signals, we focus on the ENF signal obtained directly from the power mains. This provides a most favorable condition in terms of a high signal-to-noise ratio (SNR) of the power-ENF signal. As ENF signals collected across different locations are similar to each other over time, exploration using high SNR signals may help us in understanding if ENF signals exhibit some location specific characteristics that can potentially be exploited to devise a localization protocol. Such a study may be considered an initial step towards gaining an understanding of the location estimation capabilities of ENF signals. This understanding can pave a way towards devising solutions to a more difficult problem of location estimation from audio and video recordings, as ENF signals in such recordings are present in a distorted form and at a very low SNR.

In Fig. 1(a), a plot of ENF signals extracted from three simultaneous short recordings conducted in College Park-MD, Princeton-NJ, and Atlanta-GA is shown. These three locations are part of the US eastern grid. From this figure, we observe that all three ENF signals are highly correlated at a macroscopic level; however, in the zoomed plot shown in Fig. 1(b), some differences can be seen across the three recordings. We extract these variations using a filtering mechanism, and then compare them to understand a relationship between signals recorded at different locations.

### 3.1. Signal Processing Mechanism to Extract ENF variations

As can be seen from Fig. 1(b), the variations in simultaneous ENF signals recorded across different locations of the same grid are present at high frequencies. To extract these variations, we use a high pass filtering mechanism by passing temporally aligned ENF signal, $f^{\{k\}}(n)$, recorded at $k^{th}$ location through a smoothening filter, and subtracting the resulting output signal from $f^{\{k\}}(n)$. The corresponding high pass filtered output, $f_{hp}^{\{k\}}(n)$ is given by:

$$f_{hp}^{\{k\}}(n) = f^{\{k\}}(n) - \sum_{m=-\frac{M-1}{2}}^{\frac{M-1}{2}} w(m) f^{\{k\}}(n-m) \qquad (1)$$

where $f^{\{k\}}(n)$ is the ENF value at time $n$, $w(\cdot)$ is the coefficient of the smoothening filter, and $M$ is the filter order for feature extraction, chosen as an odd number. After extracting high pass filtered signals for each location, their pair-wise cross-correlations are obtained. The pair-wise cross-correlation between any two filtered segments at time $n$ from the $k^{th}$ and the $l^{th}$ location is given by:

$$\rho_{k,l} = \frac{\sum_{p=0}^{N-1} f_{hp}^{\{k\}}(n+p) f_{hp}^{\{l\}}(n+p)}{\sqrt{\sum_{p=0}^{N-1} (f_{hp}^{\{k\}}(n+p))^2} \sqrt{\sum_{p=0}^{N-1} (f_{hp}^{\{l\}}(n+p))^2}} \qquad (2)$$

where $N$ is the length of the signal segment. A block diagram representing this signal processing mechanism is shown in Fig. 2.

### 3.2. Case Study 1: 3-Location Data on the US East Coast

In this section, we describe our experiments on a 10-hour long simultaneous recording of power data from three locations in the US

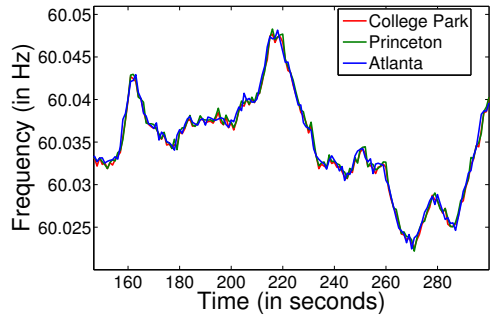


(a) Normal view

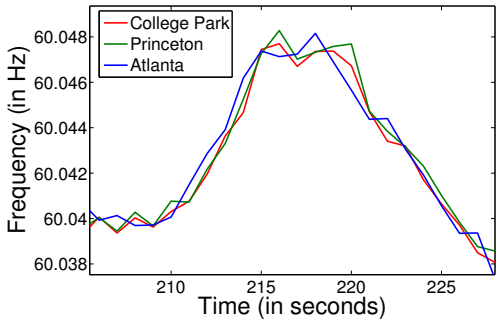


(b) Zoom view around 200-230 seconds

**Fig. 1**. Sample ENF signals extracted from recordings done in three locations in the US eastern grid of US at the same time. (figures best viewed in colors).

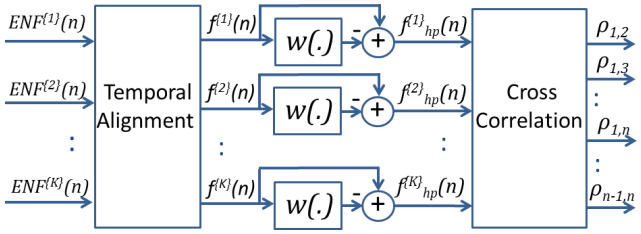


**Fig. 2**. Signal processing mechanism to explore intra-grid ENF relations.

eastern grid: College Park in Maryland, Princeton in New Jersey, and Atlanta in Georgia [7]. We use the mechanism described in Sec. 3.1 to estimate the cross-correlation between filtered ENF data from all three locations. We divide the signal into non-overlapping segments of 10 minutes each. Instantaneous frequency is estimated every 1 second using the subspace based ESPRIT [8] method, as this method provides better frequency estimation accuracy than other methods [3]. The plot of the correlation coefficients between processed ENF signals at different locations for filter order $M = 3$ is shown in Fig. 3. It can be observed from this figure that the correlation coefficient between the signals from city pairs far apart in geographical distance is less than that of between the signals from city pairs closer to each other. The correlation coefficient is approximately proportional to the distance between the cities. It is worth noting that the three cities lie approximately on a straight line on a map. Based on these observations, we derive a relationship between the correlation coefficient of the data from different locations and their geographical distances.

Let us denote Princeton-NJ by city 1, College Park-MD by city

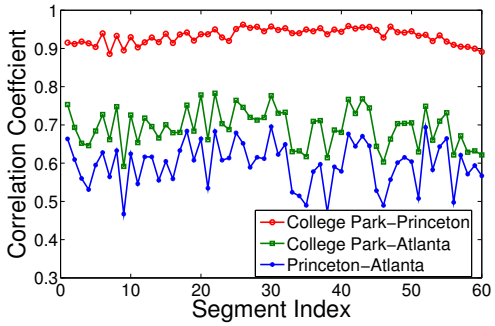


**Fig. 3**. Correlation coefficient between processed ENF signals for 3-location data on US east coast for a 600-second long query segment.

2, and Atlanta-GA by city 3. Assuming that city distance follows a linear relationship with the correlation coefficient, we use the values of correlation coefficients $\rho_{1,2}$, $\rho_{2,3}$, and corresponding city geographical distances $d_{1,2}$, $d_{2,3}$ to obtain an estimate of $d_{1,3}$ for a given observation of $\rho_{1,3}$. Based on the linear relationship, an estimate of $\widehat{d}_{1,3}$ for a given $\rho_{1,3}(n)$ can be given as:

$$\widehat{d}_{1,3} = d_{1,2} + \frac{d_{1,2} - d_{2,3}}{\rho_{1,2} - \rho_{2,3}}(\rho_{1,3} - \rho_{1,2}). \quad (3)$$

We compute the mean distance estimation error by averaging the absolute difference between $\widehat{d}_{1,3}(n)$ and true geographical distance $d_{1,3}$ for different query segments. The plot of the mean distance error in distance estimation for different segment lengths and filter orders is shown in Fig. 4(a). From this figure, we observe that when the filter order $M = 3$ is used, segment of 900 seconds provides an estimate of distance within an accuracy of 24 miles. Increasing the order of the filter worsens the distance estimates, because the use of more data in filtering of the ENF signal averages out the effects, which may have been propagated due to the finite propagation speed of the frequency disturbances across the grid. To understand the effect of temporal resolution in distance estimation, we fix $M = 3$ and plot the average distance estimation error for different duration of instantaneous frequency estimation in Fig. 4(b). From this figure, we observe that the best estimates are obtained when instantaneous frequency is estimated every 1 second. Such a phenomenon can be explained from the finite speed of signal propagation, which is empirically determined to be in the order of 500 miles for eastern grid [5]. As we increase the duration of data for instantaneous frequency estimation, the effect of the signal propagation is averaged out, leading to a decrease in the accuracy of distance estimates. Decreasing the signal duration for instantaneous frequency estimation by less than 1 second leads to an error in frequency estimation itself due to the small number of data samples available for frequency estimation.

Based on this case study on 3-location data, we see that ENF signals have the potential to be used as location-stamps. The correlation coefficient between the data recorded at an unknown location and a known location can be used to estimate the distance of the recording location from the known location. Known locations can behave as anchor nodes in designing localization protocols [9]. In the next section, we discuss another case study on 5-location data in the US eastern grid that reveals additional challenges in localization.

### 3.3. Case Study 2: 5-Location Data on the US East Coast

For this experiment, power data was collected from two more locations of Champaign in Illinois and Raleigh in North Carolina in addition to the three locations used in Sec. 3.2 in the eastern grid of US. This 5-location data is 4 hours in duration. After temporally aligning the signals, we use the mechanism described in Sec. 3.1 to estimate the correlation coefficients between the data from different city pairs for a filter order $M = 3$ and a segment length of 10

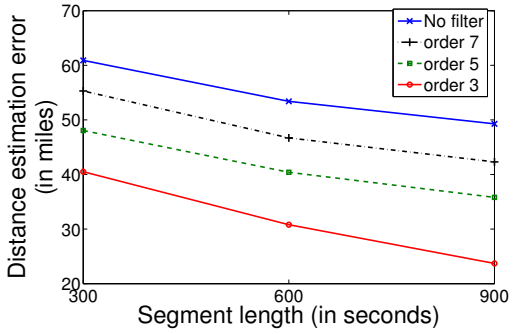


(a) For different M

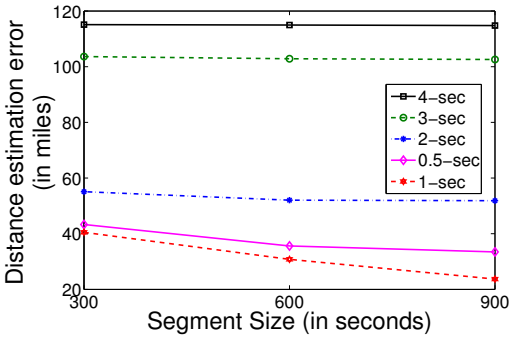


(b) Different segment duration, $M = 3$

**Fig. 4**. Mean error in distance estimation between Princeton and Atlanta using a linear relationship between correlation coefficients and distance between the cities.

minutes. The plots of the correlation coefficients between data from different cities are shown in Fig. 5. From these figures, we observe that the correlation coefficients between the data collected from cities closer to each other are higher than that of the data from cities farther apart, as was the case with 3-location data. The relative magnitude of the correlation coefficients are roughly inversely proportional with the geographical distance between the cities. For example, the distance between College Park and Princeton is the least mutual distance among all city pairs, and the correlation coefficient between the data collected from there is the highest. However, due to a different 2-dimension relation of the relative locations of the cities [10], it may not be possible to use the straight line assumption used in Sec. 3.2.

As the flow of the ENF signal over the wire lines is dependent on a variety of parameters, such as grid topology (road distance may not equal actual wire distance), grid density, etc., the correlation coefficient between data from different locations may have a complex relationship with the distance between these locations. Because of limited data available to us, we design a localization protocol without learning an explicit relationship between correlation coefficient and distance between different locations. Instead, we make use of the observation from our experiments that the pair-wise correlation between the locations far apart is less than the pair-wise correlation between the cities close to each other. Using such observations, we devise a method of half-plane intersection to estimate an unknown location of recording.

### 3.4. Half-Plane Intersection for Localization

Let us denote the location of $K$ anchor cities by $P_1 = \{x_1, y_1\}, P_1 = \{x_1, y_1\}, \ldots, P_K = \{x_K, y_K\}$. Suppose we are given ENF data collected at all anchor cities along with their known locations. Based on this information, we derive a localization protocol to estimate the unknown location of a city node (denote by A) that lies in a set of lo-

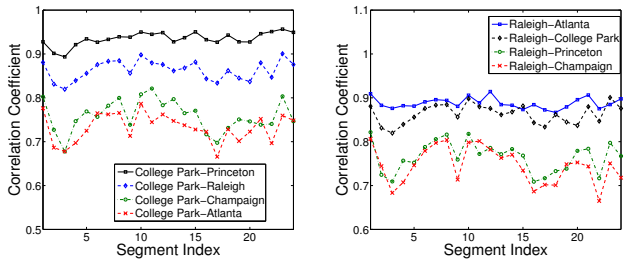


(a) Correlation with College Park data (b) Correlation with Chapel Hill data

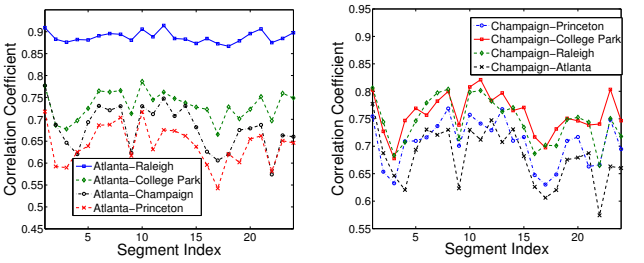


(c) Correlation with Atlanta data (d) Correlation with Champaign data

**Fig. 5**. Correlation coefficient between the processed ENF signals across different locations for 600-second query segment for 5-location data on the US East Coast

cations described by the convex hull of $P_1, P_2, \ldots, P_K$, denoted by $D$. We assume that city A's locations lies in this set. As discussed in Sec. 3.3, if the distance of $P_i$ from city A is greater than the distance of $P_j$ from city A, we generally have $\rho_{j,A} > \rho_{i,A}$. Based on this observation, we say that the location of city A lies in the half-plane described by the set of points $\widehat{P}_{i,j}$ given by:

$$\widehat{P}_{i,j} = \begin{cases} \{X : ||X - P_i||_2 > ||X - P_j||_2, X \in D\} & \text{if } \rho_{j,A} - \rho_{i,A} > 0 \\ \{X : ||X - P_i||_2 \leq ||X - P_j||_2, X \in D\} & \text{if } \rho_{j,A} - \rho_{i,A} \leq 0 \end{cases} \quad (4)$$

The conditions described in Eq. (4) are the sign bit of the difference between the correlation coefficients. These equations make use of a highly quantized information from the correlation coefficient. The conditions also provide us with hard decision boundaries of the half-plane, and does not take into account the noisy nature of pair-wise correlation coefficients. For example, when the correlation coefficients of the ENF signal of city A with $i^{th}$ and $j^{th}$ locations are very close to each other, i.e., $|\rho_{i,A} - \rho_{j,A}| < \epsilon$ for a small $\epsilon$, the confidence in assigning a half-plane to the feasible solution set $\widehat{P}_{i,j}$ is reduced in Eq.( 4). To compensate for such values of correlation coefficients, we replace the feasible set given by Eq.( 4) with the following equation with a tolerance $\epsilon$:

$$\widehat{P}_{i,j} = \begin{cases} \{X : ||X - P_i||_2 > ||X - P_j||_2, X \in D\} & \text{if } \rho_{j,A} - \rho_{i,A} > \epsilon \\ \{X : ||X - P_i||_2 \leq ||X - P_j||_2, X \in D\} & \text{if } \rho_{j,A} - \rho_{i,A} \leq \epsilon \end{cases} \quad (5)$$

Using the correlation value obtained from all the anchor nodes, the set of feasible points can be further reduced by computing the intersection of all the feasible half-planes as following:

$$\widehat{P}_A = \cap_{i,j} \widehat{P}_{i,j} \quad i, j \in \{1, 2, \ldots, K\}, i \neq j \quad (6)$$

As we have ENF data from the five locations, we use four locations as anchor cities and use the ENF data of the fifth city to estimate its location via the proposed half-plane intersection method. Due to the limited amount of data, we measure the estimation accuracy of our method by measuring the fraction of estimates that contain the actual position of the query city. If data from more anchor cities is available, location estimates can be defined using such metrics as the centroid of the feasible set.

Fig. 6 shows the plot of location estimation accuracy of different cities by considering other cities as anchor nodes. From this plot, we observe that the location estimation accuracy of some cities are very high for certain values of $\epsilon$. Location estimation accuracy of NJ and CP is approximately 100% and 85% for $\epsilon = 0.05$. For low values of $\epsilon$, the localization accuracy is less, since the hard decision rule does not provide a correct estimate when measurements are noisy. As can be seen from Fig. 5(c) and 5(d), the correlation coefficient values for different city data from Champaign-IL and Atlanta-GA are quite close to each other, and therefore it becomes difficult to use these values for assigning feasible half-plane regions. Adding more anchor nodes and placing them strategically may lead to a better location estimate.

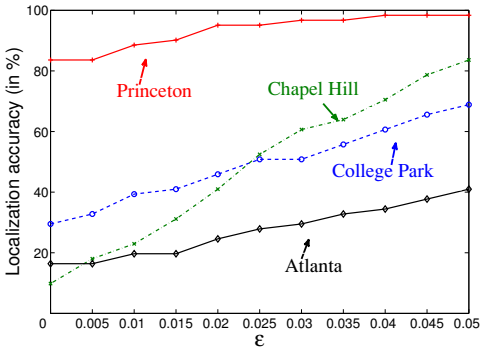


**Fig. 6**. Location estimation accuracy on 5-location US east coast data using the proposed half-plane intersection method.

## 4. DISCUSSIONS

In Sec. 3, we described the location estimation capabilities of the ENF signals. For multi-location data, we proposed a half-plane intersection method to estimate the location of an unknown recordings. The localization accuracy from this method can be improved by adding more locations as anchor nodes. The number of constraints to estimate the feasible region increases on the order of $\mathcal{O}(K^2)$ with the number of anchor cities $K$. Also, our current formulation has used highly quantized information from correlation coefficients to determine the feasible region, i.e. only the sign of the difference between the correlation coefficient of the query processed ENF signal with the ENF signals from any two anchor locations. The correlation coefficient generally carries some distance related information as was shown for 3-location data. Combination of these two aspects of correlation coefficients may lead to a better localization approach that provides a smaller set of the feasible solution as compared with the simple half-plane approach presented above. This is a part of our ongoing work.

The primary focus of this paper was to explore the uncharted application of ENF signal analysis for intra-grid location estimation of multimedia data. This first study conducts experiments on power ENF signals and provides encouraging results towards that direction. Multimedia ENF data is, however, more challenging than power ENF data because of its noisy nature. As we are utilizing the high frequency variations of the ENF signal to extract a meaningful metric for localization, the noisy nature of the ENF signal in multimedia data may make the localization task difficult. Furthermore, as shown by our experiments, location specific variations are best captured using instantaneous frequencies estimated at 1 second temporal resolution; reliable ENF signals extraction from multimedia data at such a high temporal resolution is also a research challenge. Nevertheless, the results presented in this paper demonstrate that ENF signals have a strong potential to be used as a location-stamp.

## 5. REFERENCES


[1] C. Grigoras, "Applications of ENF criterion in forensics: Audio, video, computer and telecommunication analysis," *Forensic Science International*, vol. 167, no. 2-3, pp. 136–145, April 2007.

[2] R. Garg, A. L. Varna, and M. Wu, "'Seeing ENF: natural time stamp for digital video via optical sensing and signal processing," in *Proceddings of the* $19^{th}$ *ACM International Conference on Multimedia,*, 2011, p. 2332.

[3] A. Hajj-Ahmad, R. Garg, and M. Wu, "Instantaneous frequency estimation and localization for ENF signals," in *Proceedings of the* $4^{th}$ *Annual Summit & Conferecne, APSIPA*, Dec. 2012.

[4] R. Garg, A. L. Varna, and M. Wu, "Modeling and analysis of electric network frequency signal for timestamp verification," in *IEEE International Workshop on Information Forensics and Security*, Dec. 2012.

[5] S. J. Tsai, L. Zhang, A.G. Phadke, Y. Liu, M.R. Ingram, S.C. Bell, I.S. Grant, D.T. Bradshaw, D. Lubkeman, and L. Tang, "Frequency sensitivity and electromechanical propagation simulation study in large power systems," *IEEE Transactions on Circuits and Systems*, vol. 54, no. 8, pp. 1819 –1828, Aug. 2007.

[6] M. Bollen and I. Gu, *Signal Processing of Power Quality Disturbances*, Wiley-IEEE Press, 2006.

[7] S. He, Y. Fang, and M. Luo, *Thanks for their help in data collection*.

[8] D.G. Manolakis, V. K. Ingle, and S. M. Kogon, *Statistical and Adaptive Signal Processing*, MaGraw-Hill, Inc., 2000.

[9] R. Garg, A. L. Varna, and M. Wu, "An efficient gradient descent approach for secure localization in resource constrained wireless sensor networks," *IEEE Transactions on Informations Forensics and Security*, vol. 7, no. 2, pp. 717–730, Apr. 2012.

[10] "US east coast 5-location map available online," *http://www.ece.umd.edu/ ravig/Map.html*.